Comparing Proprioceptive Acuity in the Arm between Joint Space and Task Space

Sean M. Sketch, Amy J. Bastian, and Allison M. Okamura

Abstract— **Proprioception—the sense of one's body position and movement, without the aid of vision—plays a critical role in human motor control, allowing us to adeptly move our bodies through a high-dimensional task space. The relationship between joint space and task space with regard to proprioception has not been studied in the general population. This work begins to explore the relationship between proprioceptive acuity—the combination of accuracy and precision—in joint space and task space, focusing on the elbow, shoulder, and hand of the arm in single-joint (joint-space) and integrated multi-joint (task-space) active position-matching tests with a planar, robotic arm support. Our results reveal a strong correlation between joint-space proprioception at the shoulder and elbow and task-space proprioception at the hand. However, when joint-space proprioceptive error is propagated through a model of the arm's planar kinematics, it agrees poorly with the proprioceptive error measured explicitly in task space. Task-space proprioception exhibits greater accuracy than joint-space proprioception, as would be expected given the greater biological relevance of a planar reach compared to an isolated joint movement. Task-space and joint-space proprioception also differ in directional precision, exhibiting the greatest variance along nearly orthogonal axes, approximately aligned with the sagittal and frontal body planes. These findings have implications for the diagnosis of sensorimotor impairment and the development of movement therapies following neurological injury.**

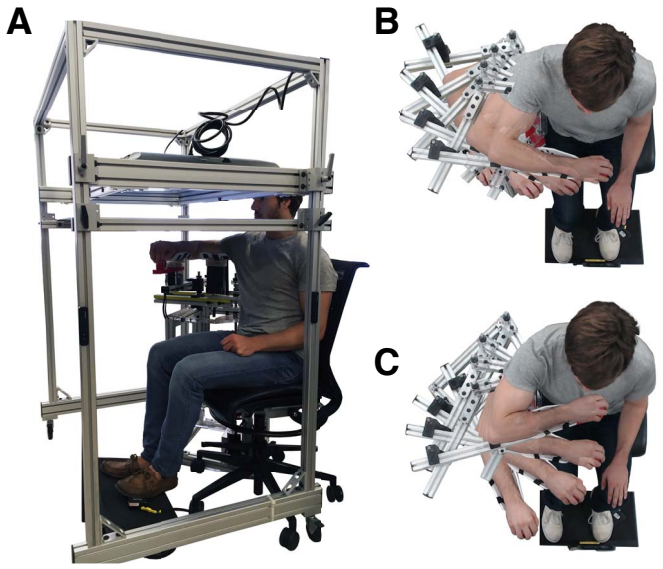

Fig. 1. **chARM exoskeleton robot.** We developed a robotic arm support—the chARM exoskeleton—for testing proprioception. **A:** A user supported by the exoskeleton while viewing a target on the mirror display. **B & C:** Overhead views of the exoskeleton during isolated movement about the shoulder and elbow, respectively.

I. Motivation

Sensorimotor control dictates how we interact with the world around us. The more accurate and precise this control, the more adeptly we are able to navigate our bodies through a high-dimensional task space. Sensing and estimation are central components of sensorimotor control; together, they close the loop on motor control [1]. A significant yet poorly understood part of sensing and estimation is proprioception, which provides a sense of the body's position and movement in space without the aid of vision. Here we seek to understand the relationship between proprioception in joint space—where we find the majority of the mechanoreceptors that contribute to proprioception [2]—and task space—where we perform control for activities of daily living (ADLs). Establishing this relationship is an important first step towards a quantitative link between proprioception and sensorimotor control. Such a link might allow clinicians to understand the relative contributions of sensory and motor impairment to the difficulty with ADLs that often follows neurological injury. This could enable more personalized design of movement therapies and assistive devices.

S. M. Sketch and A. M. Okamura are with the Department of Mechanical Engineering at Stanford University, Stanford, CA, 94035 USA (e-mail: ssketch@stanford.edu; aokamura@stanford.edu)

A. J. Bastian is with the Department of Neuroscience at The Johns Hopkins School of Medicine and the Kennedy Krieger Institute, Baltimore, MD, 21205 USA (e-mail: bastian@kennedykrieger.org)

This work was supported by the Stanford Neurosciences Institute's Stroke Collaborative Action Network and a Pfeiffer Research Foundation fellowship (a Stanford Interdisciplinary Graduate Fellowship affiliated with the Stanford Neurosciences Institute) to SMS.

II. Prior Work

Proprioception encompasses senses of both position and movement. In this work, we focus on position sense, specifically in the arm. Given the central role that proprioception plays in sensorimotor control (e.g., preventing drift and additive errors during sequential movements [3], [4]), a large body of research has been done to quantify the acuity—defined here as the combination of accuracy and precision—of position sense in the arm.

A. Joint Space

Joint position sense is typically characterized by angular accuracy and precision parameters. Precision effectively remains constant over a joint's workspace. However, there appears to be a linear relationship between accuracy—specifically, the signed difference between (proprioceptively) perceived and actual position—and joint angle at both the shoulder and elbow [5], [6]. The details concerning this

linear relationship depend on other kinematic parameters. For example, Fuentes and Bastian [7] showed that elbow flexion angle is overestimated close to joint limits when the shoulder is abducted and supported against gravity. Other studies assessing shoulder position sense found accuracy to increase near the extremes of the joint's range of motion [8]–[10].

There is debate over acuity differences between the shoulder and elbow. Barrack et al. [11] and Aydin et al. [12] demonstrated that proprioceptive acuity decreases with joint mobility. Those joints with less biomechanical stability (e.g., the shoulder), potentially due to ligament laxity, exhibit less acute position sense. In contrast, multiple studies have provided evidence against any significant difference [5], [6], [13], [14]. They suggest that the central nervous system is able to overcome anatomical differences between the joints when estimating position.

The understanding of joint position sense is complicated when active movement and muscular effort are considered. During active movement, the brain's predictive model—hypothesized to reside in the cerebellum—uses efference copy, or knowledge of motor commands, to improve estimation of the body's state [15]–[17]. That said, efference copy can exist without movement—as in isometric cases—and joint position sense has been shown to improve with increased torque at a joint, such as when the shoulder is abducted against gravity [18]. Since joint torques work to stabilize the joint by increasing effective stiffness, this result is consistent with [12].

B. Task Space

Position sense at the multi-joint, task-space level is often quantified in a manner amenable to clinical diagnosis of impairment. For example, Dukelow et al. [19] report a (reachable) workspace contraction parameter for patients who suffered a stroke. Embedded in this analysis is information that enhances our fundamental understanding of proprioception. For example, it is widely accepted that proprioception varies across task space (e.g., in the plane [20]). Specifically, there is significant evidence of greater proprioceptive error with increasing distance from the body [19], [21], [22]. This supports the hypothesis that joint-level errors are propagated through the arm's forward kinematics into task space [13], [14], [23].

C. Joint Space vs. Task Space

Although several studies allude to the importance of understanding the relationship between proprioception in joint and task space [22], [24], very few have rigorously analyzed the connection. Tripp et al. [17], investigated position-sense acuity at the shoulder, elbow, and wrist in highly trained baseball players performing an overhead throwing motion. Using principal component analysis they found that joints more proximal to the body (e.g., the shoulder) contribute more to task-space proprioception than more distal joints. That is, a small proprioceptive deficit at the shoulder is more deleterious to task-space proprioceptive acuity than a similar deficit at the elbow. Although such findings help to form a holistic understanding of position sense, the investigational separation between joint and task space remains. Nearly all proprioceptive assessments are performed in either joint or task space, not both. Thus, our work studies the relationship between joint- and task-space position sense in a general population, using the commonly studied center-out planar-reaching paradigm.

III. Methods

We assessed proprioception using position-matching tasks in which subjects actively moved single or multiple joints to match target positions. For precise measurement and resetting of arm position during these tasks, we employed a planar, two-degree-of-freedom robotic exoskeleton. For visualization of targets and instructions associated with the tasks, we augmented the exoskeleton with a graphical display aligned with the arm's position. Eighteen healthy subjects volunteered to participate in the experiment. Data from twelve of these subjects were analyzed using standard statistical techniques.

A. Evaluation Apparatus

Many devices exist for assessing motor and sensory abilities in the arm. Scott and Dukelow summarize the offerings and discuss their potential for neurorehabilitation in [25]. Driven by a need to customize an apparatus for our desired studies, we developed our own robotic arm support. Inspired by the KINARM exoskeleton (©BKIN Technologies [19]), we refer to this robot as the chARM exoskeleton (Fig. 1).

The chARM exoskeleton was designed to be high-fidelity, adjustable, and relatively low-cost. It consists of an arm-supporting parallelogram four-bar linkage driven by two ground-mounted motors (Maxon RE 65 DC) through a 17:1 capstan-drive transmission. The motors are powered by a 320-Watt supply—governed by a Sensoray 826 PCIe board—through an Advanced Motion Controls 25A20 PWM servo drive. Accounting for voltage and current limits in all components of the system, the linkage can provide peak torques of nearly 40 Nm and continuous torques of nearly 13.5 Nm at both the shoulder and elbow. For safety reasons, the exoskeleton's software limits all torques to 12 Nm; this translates to approximately 35 N (just under 8 lbs) of force at the hand for an average person, in the middle of the workspace. There is also an emergency-stop button within reach of the experimenter and press-to-power foot pedal ("deadman's switch") within reach of the user at all times. Motor-mounted 500 count-per-revolution encoders (Maxon HEDL 5540) track angular position of the linkage's shoulder and elbow with a resolution of 0.01 degrees, when accounting for the capstan ratio.

chARM is constructed primarily of 80-20 aluminum framing/connectors and laser-cut acrylic. Shafts are steel, and high-load-bearing portions of the linkage (i.e., those close to the shoulder axis) are reinforced with custom-machined aluminum-alloy plates. The links supporting the upper arm and forearm are connected with custom-machined Delrin

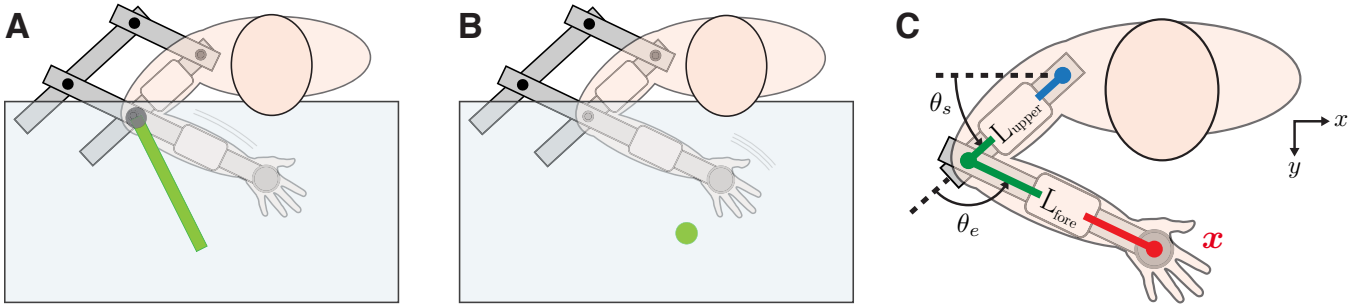

Fig. 2. **Schematic of position-matching tests.** In both joint-space and task-space tests, the arm is hidden beneath the mirror display. Tests *with vision* display the arm—specifically, the upper arm or forearm in joint-space tests and the hand in task-space tests—as an on-screen avatar. The display is calibrated to the exoskeleton such that this avatar corresponds exactly to the subject's arm. **A:** Joint-space matching at the elbow. The target is a green cylinder (sized to match the subject's forearm) that originates from and rotates about the elbow. The shoulder is locked to prevent motion of the upper arm. Joint-space matching at the shoulder is performed similarly, with elbow locked to prevent motion of the forearm relative to the upper arm. **B:** Task-space matching to one of eight targets. Both joints are unlocked to allow unconstrained motion in the plane, within the exoskeleton's workspace. **C:** Variables measured during the experiment. θ_s and θ_e are shoulder and elbow angle, respectively. $\boldsymbol{x}$ is hand position in the plane. L_{upper} and L_{fore} are, respectively, upper arm length—measured from shoulder joint (blue) to elbow joint (green)—and forearm length—measured from elbow joint (blue) to where the hand grips the exoskeleton's end-effector (red). Portions of the four-bar linkage have been removed for clarity.

brackets, allowing the forearm link to slide (and lock in place) relative to the upper arm link. Elevated upper arm and forearm supports are made of plastic-coated wood, topped with custom 3D-printed adjustable trays. Combined with the four-bar linkage's variable size, these three-degree-of-freedom trays (translation along and orthogonal to the links plus rotation about their center) make chARM adjustable for a wide range of subjects. The end-effector is a 3-D printed ball that can be held by a subject during testing. Each degree of freedom can be locked independently. An adjustable-height chair and adjustable-height footrest are connected to the exoskeleton frame.

Control and visualization software for chARM is programmed in C++ using Qt and the CHAI3D haptic and graphic simulation framework [26]. It provides the experimenter with a view of the exoskeleton, as well as interfaces for updating subject parameters and manually controlling the robot. All control—in both joint and task space—is PID; the proportional, integral, and derivative gains can be increased for heavier subjects via a pop-up GUI. Control and graphic updates are performed at greater than 20,000 Hz and 10 Hz, respectively.

To display a graphic of the arm that spatially aligns with the arm of a subject seated in the exoskeleton, we use a mirror display. Like the exoskeleton, the display's frame is constructed of 80-20 aluminum framing/connectors. It supports a 46-inch wide-screen television and slightly larger sheet of mirrored acrylic. The television faces downward at the acrylic so that displayed graphics are reflected in the mirrored surface. Locking slides on the frame's vertical supports adjust the height of both the television and mirror. To guarantee that graphics appear in the plane of the subject's arm, the mirror is positioned midway between the exoskeleton's arm trays and the screen of the television. Locking wheels allow the frame to be moved into place once the subject is seated in the exoskeleton. Laser pointers rigidly attached to the frame allow for repeatable alignment with respect to the exoskeleton, guaranteeing correspondence between the origin and axes of the graphical and real world.

B. Experimental Protocol

Subjects performed joint-space and task-space active position-matching tasks as described below. This study was part of a larger quantitative assessment of proprioception, which lasted 1.5–2 hours, and could be performed over two days if requested by the subject. This larger assessment included two additional tests: (1) single-joint assessments at the shoulder and elbow using a psychometric adaptive staircase procedure, similar to that of [27], and (2) passive single-joint matching at the shoulder and elbow, during which the subject moved an arm avatar to coincide with their hidden arm. Results from these additional tests are not presented here.

Prior to the assessment, subjects were fitted to the chARM exoskeleton. First, with the mirror display moved aside, a subject sat in the chair, the height of which was adjusted to align the subject's shoulder plane (shoulder at 90° abduction) with the plane of the exoskeleton's arm trays (see subject positioning in Fig. 1A). Second, the subject rested upper arm and forearm in the trays and was asked to shift seating position in the chair until the shoulder joint aligned with the main (shoulder) axis of the exoskeleton. Third, the experimenter adjusted the dimensions of the four-bar linkage, sliding and locking its forearm link relative to the upper arm link—while maintaining the linkage's parallelogram structure—until the elbow axis aligned with the subject's elbow joint. Fourth, the experimenter adjusted the exoskeleton's arm trays (in all degrees of freedom) to provide comfortable support of the arm segments and a natural grip of the linkage's end-effector. Finally, the experimenter measured the subject's arm parameters (upper arm length L_{upper} and forearm length L_{fore}) from the exoskeleton as diagrammed in Fig. 2C; these were recorded in the experiment software to guarantee appropriately sized graphics. Given that joint position sense at the shoulder does not vary with head, neck, or trunk

position/orientation [18], [28], subjects were not restrained in the chair. However, they were instructed to not shift their seating position in the chair during a test.

During the assessment, joint-space tests preceded task-space tests. Within a joint-space test, shoulder trials preceded elbow trials. During a trial, subjects were allowed as much time as necessary to complete the task. Between tests, subjects received a break of at least two minutes. During longer tests, subjects received a break of at least one minute, halfway through the test. As will be evident from the descriptions that follow, our position-matching tests did not require the subject to rely on visual or motor memory (e.g., memory of a held position).

1) Joint-Space Active Position Matching: In joint-space active position matching (Fig. 2A), the subject moved a single arm segment to align with an on-screen cylinder. The cylinder originated from and rotated about the joint being tested and was length-matched to the associated arm segment (L_{upper} when testing the shoulder, L_{fore} when testing the elbow). For each joint, the target cylinder appeared at one of two angles: 30° or 50° for the shoulder, 70° or 110° for the elbow. These angles were selected to be near the center of a healthy subject's range of motion (avoiding phenomena near the joint limits [7]), within chARM's physical workspace, and within the visual display space. Each target angle was presented a total of six times; the order of the twelve trials was randomized for each joint. Each joint was tested twice, once with vision of the arm's movement—provided by a semi-transparent ghost cylinder that moved with the subject's arm—and once without vision; this order was pseudo-randomized.

Prior to each trial, the subject's position sense was visually grounded by displaying the ghost cylinder at an angle between the target angles—40° for the shoulder, 90° for the elbow; the arm was then moved without vision to a different starting angle—15° for the shoulder, 125° for the elbow. This prevented proprioceptive drift over the course of the test. During the test, movement of the untested segment was physically prevented by the exoskeleton. For shoulder tests, the elbow was locked at approximately 110°. For elbow tests, the shoulder was locked at approximately 60°.

2) Task-Space Active Position Matching: In task-space active position matching (Fig. 2B), the subject moved the end-effector of the (unconstrained) exoskeleton—and therefore their hand—to align with an on-screen sphere, similar to a center-out planar reach. The target sphere was positioned at one of eight positions equally spaced around a circle. The circle's center point was approximately 30 cm in front of the subject's right shoulder and its radius was 10 cm. The center point and radius were selected to maximize the range of subjects (with different arm segment lengths) able to reach all targets and remain within chARM's workspace. Each target position was presented a total of six times for a total of 48 trials. Presentation order was pseudo-randomized such that each target appeared once per eight trials.

As in joint space, this procedure was tested with and without vision of the arm's movement—provided by a semi-transparent ghost sphere that moved with the chARM end-effector. Vision order (with and without vision) was pseudo-randomized and the subject's position sense was visually grounded prior to each trial by displaying the ghost sphere at the center point of the target circle.

C. Subjects

Eighteen healthy subjects volunteered for this study. Six of these either did not complete the experiment or do not have their results reported here. Two subjects did not participate because they were too small or too large to use the apparatus to see and reach all targets. A second subject was too small to reach all task-space targets while in the exoskeleton. A third subject was unable to find time to return to the lab to complete the final test of the experiment. A fourth subject's shoulder and elbow became misaligned with the exoskeleton's joint axes over the course of the experiment. A fifth subject's language barrier prevented him from understanding experimental instructions. The sixth subject was ambidextrous; we only analyzed and report results from right-hand-dominant subjects. The remaining twelve subjects—six male, six female, all right-hand dominant—were of mean age 25 ± 5 years with upper arm length L_{upper} of 9.6 ± 0.9 inches and forearm length L_{fore} of 13.4 ± 1.0 inches. Each subject completed the tests in a unique order. The experimental protocol was approved by the Stanford University Institutional Review Board and all participants gave informed consent.

D. Data Analysis

In the equations that follow, vectors are typeset in bold. Joint-space equations that do not reference a specific joint (Eqns. 1–3) are applied to both the shoulder and elbow.

1) Adjustment Using With-Vision Data: To remove errors due to vision and movement from the results of position-matching tests, we adjusted *without-vision* data (denoted by subscript "−vision") using *with-vision* data (denoted by subscript "+vision") as follows:

$$\begin{aligned} \theta_{\text{corr}} &= \theta_{-\text{vision}} - \overline{\Delta\theta}_{+\text{vision}} \\ \boldsymbol{x}_{\text{corr}} &= \boldsymbol{x}_{-\text{vision}} - \overline{\Delta\boldsymbol{x}}_{+\text{vision}} \end{aligned} \tag{1}$$

$\overline{\Delta\theta}$ and $\overline{\Delta\boldsymbol{x}}$ are mean errors and are defined in Eqns. 2 below. This correction lumps error in position sense with temporally integrated errors in the brain's predictive model; in the *with-vision* case, visual feedback corrects for the accumulation of errors from the predictive model. Given the exoskeleton's anisotropic dynamics (e.g., due to friction), we assume that the brain does not rely on predictive modeling during these position-matching tests; thus, post-correction errors can be completely attributed to proprioception. Unless otherwise noted, all results presented in this work are computed from adjusted *without-vision* data.

2) Statistical Computations: Using the adjusted data, we calculated summary statistics for each matching angle in joint space—θ_{targ}, two per joint as described in Section III-B.1—and matching position in task space—$\boldsymbol{x}_{\text{targ}}$, eight in total as described in Section III-B.2. Mean deviation or bias,

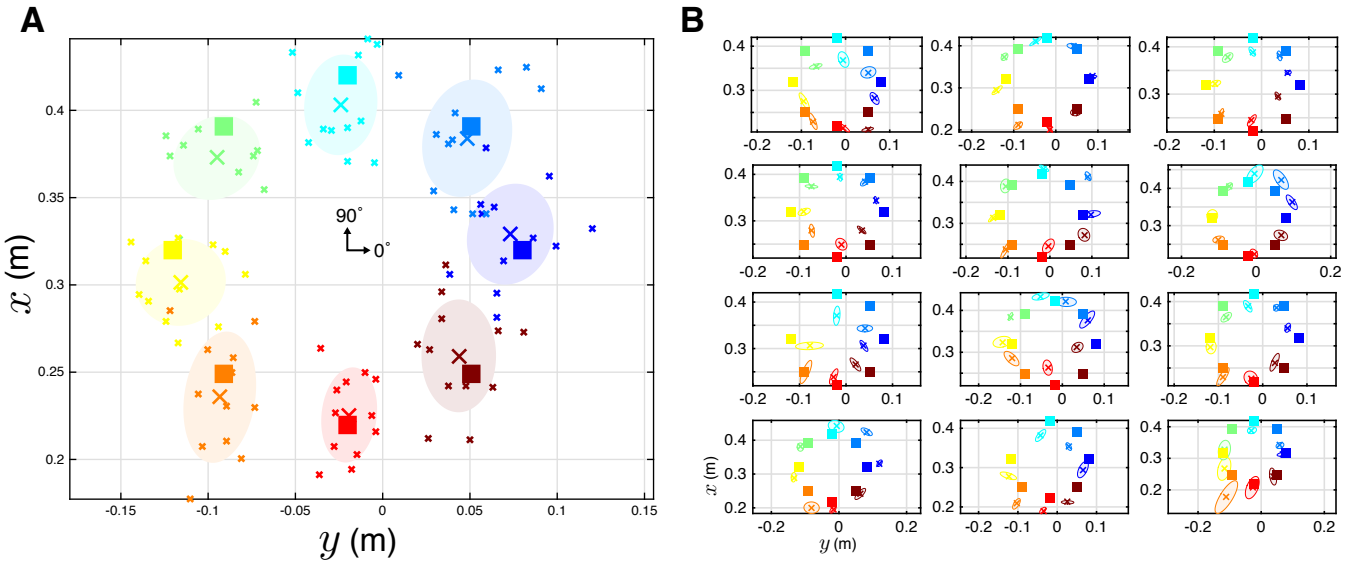

Fig. 3. **Task-space matching errors. A:** Group statistics for the eight task-space targets (targets represented by filled colored squares). Large and small x's correspond to group and subject means, respectively, when matching the targets *without vision*. Both have been adjusted using mean data from *with-vision* matching tests. The shaded area surrounding each group mean is a one-standard-deviation error ellipse; it assumes that the data is normally distributed. **B:** Individual results for all twelve subjects. Statistics display idiosyncratic variation between subjects. Two subjects were unable to reach the 135° target due to the exoskeleton's limited workspace; this target does not appear on their plots and their data for this target was not included in the group analysis.

represented by $\overline{\Delta\theta}$ in joint space and $\overline{\Delta \boldsymbol{x}}$ in task space, is calculated as follows:

$$\begin{aligned} \overline{\Delta\theta} &= \bar{\theta} - \theta_{\text{targ}} \\ \overline{\Delta \boldsymbol{x}} &= \bar{\boldsymbol{x}} - \boldsymbol{x}_{\text{targ}} \end{aligned} \tag{2}$$

where $\bar{a} = \frac{1}{n}\sum_{i=1}^{n} a_i$ is the mean of quantity a, either a set of joint angles or task-space positions thought by the subject to match the target. This is an accuracy statistic. The corresponding precision statistic is standard deviation σ_θ in joint space and covariance matrix $\Sigma_{\boldsymbol{x}}$ in task space:

$$\begin{aligned} \sigma_\theta &= \sqrt{\frac{1}{n-1}\sum_{i=1}^{n}\left(\theta_i - \bar{\theta}\right)^2} \\ \Sigma_{\boldsymbol{x}} &= \begin{bmatrix} \Sigma_{xx} & \Sigma_{xy} \\ \Sigma_{yx} & \Sigma_{yy} \end{bmatrix} \end{aligned} \tag{3}$$

where $\Sigma_{ab} = \frac{1}{n-1}\sum_{i=1}^{n}\left(a_i - \bar{a}\right)\left(b_i - \bar{b}\right)$ is the covariance of quantities a and b. When accuracy and precision are calculated for an individual subject, $n = 6$, the number of trials for each target. For group statistics, $n = 72$, the number of trials across all twelve subjects.

3) Error Propagation from Joint Space to Task Space: To compare joint-space and task-space accuracy and precision, we propagated joint-space statistics into task space. First, we modeled the arm as a revolute-revolute (RR) robot constrained to move in the plane of the shoulder [29]–[32]. This gives the following nonlinear forward kinematics:

$$\boldsymbol{x} = f\left(\boldsymbol{\theta}\right) = \begin{bmatrix} \text{L}_{\text{upper}}\cos\left(\theta_s\right) + \text{L}_{\text{fore}}\cos\left(\theta_s + \theta_e\right) \\ \text{L}_{\text{upper}}\sin\left(\theta_s\right) + \text{L}_{\text{fore}}\sin\left(\theta_s + \theta_e\right) \end{bmatrix} \tag{4}$$

where $\boldsymbol{x} = [x\ y]^T$ is hand position and $\boldsymbol{\theta} = [\theta_s\ \theta_e]^T$ is the vector of shoulder and elbow joint angles. Joint angles θ_s and θ_e and arm segment lengths L_{upper} and L_{fore} are defined in Fig. 2C. Assuming only positive elbow angles, the inverse kinematics are uniquely defined as $\boldsymbol{\theta} = f^{-1}\left(\boldsymbol{x}\right)$.

Using forward and inverse kinematics, we propagated accuracy from joint space into task space, for a given $\boldsymbol{x}_{\text{targ}}$, as follows:

$$\overline{\Delta \boldsymbol{x}} = f\left(\boldsymbol{\theta}_{\text{targ}} + \overline{\Delta\boldsymbol{\theta}}\right) - \boldsymbol{x}_{\text{targ}} \tag{5}$$

where $\boldsymbol{\theta}_{\text{targ}} = f^{-1}\left(\boldsymbol{x}_{\text{targ}}\right)$ and $\overline{\Delta\boldsymbol{\theta}} = [\overline{\Delta\theta}_s\ \overline{\Delta\theta}_e]^T$ is interpolated from joint-space accuracy statistics at $\boldsymbol{\theta}_{\text{targ}}$, assuming a linear relationship between joint angle and its accuracy [5], [6]. To propagate precision from joint space into task space, we first linearized Eqn. 4 using the Jacobian matrix J:

$$\boldsymbol{x} \approx \boldsymbol{x}_0 + J\boldsymbol{\theta}$$

This yields the following relationship between joint-space and task-space covariance matrices [33]:

$$\Sigma_{\boldsymbol{x}} \approx J\Sigma_{\boldsymbol{\theta}}J^T \tag{6}$$

For the joint-space covariance matrix, we assumed independence between variance at the shoulder and elbow (i.e., a diagonal structure to $\Sigma_{\boldsymbol{\theta}}$):

$$\Sigma_{\boldsymbol{\theta}} = \begin{bmatrix} \sigma_{\theta_s}^2 & 0 \\ 0 & \sigma_{\theta_e}^2 \end{bmatrix}$$

σ_{θ_s} and σ_{θ_e} are averaged from joint-space precision statistics.

4) Significance Tests: We tested for significant differences between task-space and propagated joint-space error using Hotelling's two-sample test [34], a multivariate generalization of Student's two-sample t-test. We assumed indepen-

dence and heteroscedasticity (unequal covariance matrices) between the joint- and task-space datasets and performed the test at the group level, for each target independently. Because joint-space error only exists in task space as a set of bias vectors and covariance matrices (bivariate Gaussian distributions, computed via Eqns. 5 and 6), we generated explicit joint-space data for each target via Monte Carlo simulation (i.e., by randomly drawing $n = 72$ x-y pairs from the distribution). We compared this generated data to data recorded from task-space position-matching tests.

5) Proprioceptive Acuity Score: To assess the correlation between joint-space and task-space proprioception, we summarized each subject's accuracy and precision statistics into scalar acuity metrics, $m_{\boldsymbol{\theta}}$ for joint space and $m_{\boldsymbol{x}}$ for task space. In joint space, we averaged across the two joints and two target angles:

$$m_{\boldsymbol{\theta}} = \left(\frac{1}{2} \sum_{j \in J} \left(\frac{1}{2} \sum_{i \in \Theta_j} \sigma_{\theta_{ji}} \left(1 + \frac{\overline{\Delta\theta}_{ji}}{i} \right) \right) \right)^{-1} \tag{7}$$

where $J = \{\text{shoulder}, \text{elbow}\}$ and $\Theta_j = \{30^\circ, 50^\circ\}$ for the shoulder and $\{70^\circ, 110^\circ\}$ for the elbow. $\overline{\Delta\theta}_{ji}$ and $\sigma_{\theta_{ji}}$ are the accuracy and precision statistics, respectively, for joint j at target angle i. In task space, with both joints free to move, we averaged across the eight targets positions:

$$m_{\boldsymbol{x}} = \left(\frac{1}{8} \sum_{\boldsymbol{x} \in \boldsymbol{X}} A_{\boldsymbol{x}} \left(1 + \frac{\left\| \overline{\Delta \boldsymbol{x}} \right\|}{d} \right) \right)^{-1} \tag{8}$$

where $\boldsymbol{X}$ contains all eight $\boldsymbol{x} = [x \ y]^T$ target positions, $A_{\boldsymbol{x}}$ corresponds to the area of the one-standard-deviation ellipse associated with target $\boldsymbol{x}$, and $d = 10$ cm is the radius of the circle of targets. Since greater error corresponds to poorer acuity, the final reciprocal taken in both Eqns. 7 and 8 translates error to acuity.

IV. Results

Results from tests *with vision*—both in joint and task space—were nearly identical across subjects; bias and variance were effectively zero, indicative of "perfect" motor control. *Without vision*, we observed large variation across subjects (Fig. 3B). The results below were computed from data averaged across the group. We first independently present results from the joint-space and task-space matching tests. We then compare results in joint and task space by propagating the joint-space statistics into two-dimensional task space, as described in Section III-D.3.

A. Joint Space

Joint-space statistics are presented in Table I. Across target angles, precision is relatively constant. However, accuracy is highly variable. Generally, angles are under- and overestimated at the shoulder and elbow, respectively.

B. Task Space

Task-space statistics are summarized in Fig. 3. There was a high degree of variation across subjects. When grouped, biases are relatively small but significantly different from zero for all but the 45° and 270° targets ($p < 0.05$, Hotelling's one-sample test). Error ellipses appear similar across the workspace. Across targets, the largest variance is generally aligned with y, along the sagittal axis.

TABLE I
Joint-Space Matching Errors

	SHOULDER		ELBOW	
θ_{targ}	30°	50°	70°	110°
$\overline{\Delta\theta}$	-3.7°	-7.2°	9.3°	0.3°
σ_θ	5.7°	4.9°	4.6°	4.1°

C. Joint Space vs. Task Space

Fig. 4 compares task-space (blue) and propagated joint-space (red) error statistics in two dimensions. For all but the 0° target, task-space bias is significantly smaller than joint-space bias ($p < 0.005$, Hotelling's two-sample test). Overall, joint-space means appear systematically shifted towards the upper right of the workspace. Only the error ellipses associated with the 0° and 135° targets are significantly different in size between joint space and task space ($p < 0.05$, Wilcoxon signed-rank test). However, those ellipses propagated from joint-space are consistently rotated clockwise relative to the task-space ellipses.

Fig. 5 provides evidence for a strong linear correlation between joint and task-space acuity scores (Pearson correlation coefficient $\rho = 0.79$, $p < 0.005$). Five subjects' scores lie on the least-squares line. However, there are several large residuals, suggesting limitations in this specific error-propagation model between joint and task space.

V. Discussion

This work investigates the relationship between joint-space and task-space proprioception—specifically, the acuity of position sense—in the commonly studied center-out planar-reaching paradigm. Joint-space statistics are presented for the sake of comparison to task-space statistics, when propagated into task space. Analysis of unpropagated joint-space statistics is left to future work.

In our task-space test, the circle of targets is close to the subject's body and centered relative to the torso; subjects are reaching to targets near the center of their arm's workspace. Given this, we expected task-space data to reveal small bias (high accuracy) across all targets. Fig. 3A shows that this hypothesis appears to hold true when results are averaged across subjects. However, it does not hold for individual subjects; Fig. 3B shows that subjects' task-space errors are idiosyncratic, in agreement with [20].

Group-averaged biases are significantly different from zero for all but the 45° and 270° targets. Movement to the 45° target requires minimal coupling between the shoulder and elbow. Starting from the center of the target circle, it is essentially an elbow extension. Given visual grounding and

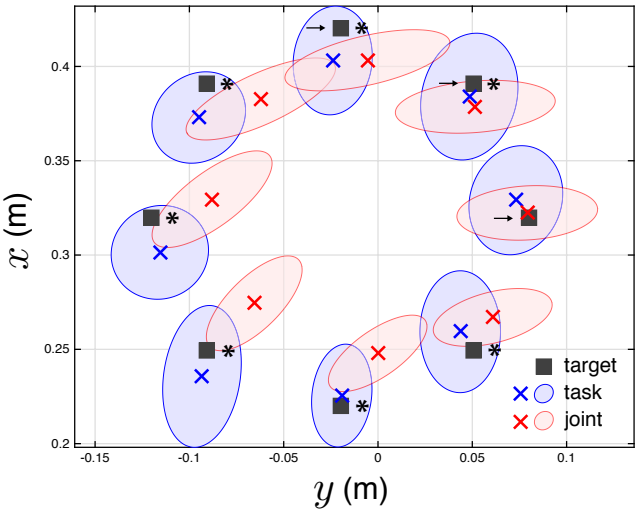

Fig. 4. **Comparison of joint-space and task-space proprioceptive error.** Blue x's and error ellipses represent statistics from the task-space *without-vision* matching test. Red x's and error ellipses represent statistics from the joint-space *without-vision* matching test, propagated into task space. Both sets of statistics have been adjusted using mean data from *with-vision* tests. Targets are represented by gray filled squares. For targets with an asterisk *, there is a statistically significant difference between joint- and task-space distributions ($p < 0.005$, Hotelling's two-sample test). For reference, those targets marked with an arrow $\rightarrow$ are associated with p-values of 0.05, 0.0003, and 0.002, proceeding counterclockwise. p-values for the remainder of targets are effectively zero.

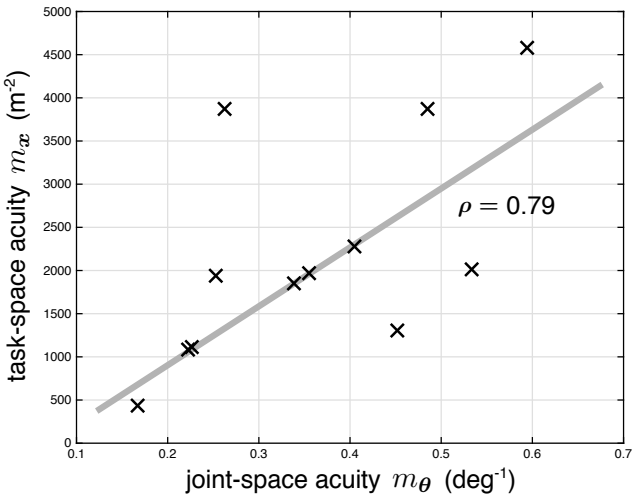

Fig. 5. **Correlation between joint-space and task-space proprioceptive acuity.** The gray line represents a least-squares best fit to the acuity data. The corresponding Pearson correlation coefficient is $\rho = 0.79$ ($p < 0.005$, Student's t-test), suggesting a strong but not perfectly linear relationship between the acuity scores defined in Eqns. 7 and 8.

lack of shoulder movement, we conclude that the resultant task-space error is only a function of error at the elbow, not a compounding of errors from the shoulder and elbow; this explains the high accuracy. Although movement to the 270° target does require joint coupling (shoulder extension plus elbow flexion), the target is the closest of all eight targets to the subject's torso. Given the evidence of greater proprioceptive error with increasing distance from the body [19], [21], [22], it is expected that matching to this target would be most accurate.

Like accuracy, task-space precision is similar across the workspace (again, for group-averaged data, not individual subjects); task-space error ellipses are consistent in both size and orientation. This consistency agrees with findings that joint-space precision does not vary significantly across joint range of motion. However, for all targets the direction of largest variance is more aligned with y (the sagittal axis) than x. This result is in disagreement with previous work using the KINARM exoskeleton [19]. It could possibly be explained by the anisotropy of our exoskeleton's dynamics. A passive version of task-space position matching, or control-based compensation for robot dynamics, might reveal a change in this trend; both are opportunities for future work. Alternatively, the change in ellipse orientation could be an artifact of our position-matching protocol, which deviates from previous studies [19], [22] by not requiring inter-arm matching. A unique testing protocol yielding unique proprioceptive errors is consistent with theory that the human neuromuscular system both optimally controls movement and optimally estimates limb state [1], [31].

When comparing task-space acuity to joint-space acuity propagated into task space, the difference in accuracy is immediately apparent. The increased accuracy in task space agrees with results from both behavioral research [7] and neural recording studies. The brain appears to encode arm state in terms of endpoint position instead of joint angles [35], [36]. This suggests that clinicians should assess proprioception in task space—perhaps via a rudimentary position-matching test—instead of at the joint level, as is most commonly done now. Of course, the strong correlation between proprioceptive acuity in joint space and task space makes it possible to reasonably predict *overall* task-space acuity from a measure of *overall* joint-space acuity. Future work will aim to understand why specific subjects might deviate significantly from such a predictive model.

Differences in precision between joint space and task space manifest in direction rather than magnitude. We characterize the magnitude of position-matching precision (for a given target) based on the area enclosed by the one-standard-deviation error ellipse; this area is a direction-agnostic characterization of the spread of the matching data. These areas are only significantly different for two of the targets. However, the orientations of joint-space and task-space ellipses are visibly different across all targets. As noted above, this could be an artifact of the neuromuscular system applying optimal control and estimation in the face of unique testing protocol. This will be the subject of future work.

A portion of the difference in accuracy between joint space and task space, as well as the difference in precision—specifically, the orientation of error ellipses—is likely due to missing elements in our model of error propagation from joint space to task space. For example, we do not account for off-diagonal entries in the joint-space covariance matrix. Moreover, we assume that joint-space bias is only a linear

function of the biased joint angle. As described in Section II, joint-space accuracy is likely dependent on a number of kinematic parameters, such as the configuration of neighboring joints. Future work will quantify how proprioceptive acuity at the joints varies with overall arm state, as well as how this variation impacts task-space sensorimotor control.

ACKNOWLEDGMENTS

The authors thank Lingjie "Kimi" Kong, Cole Simpson, Brian Su, Brice Dudley, Javier Reyna, and Joey Greer for their extensive help with design and programming of the chARM exoskeleton.

REFERENCES

[1] R. Shadmehr and J. W. Krakauer, "A computational neuroanatomy for motor control," *Experimental Brain Research*, vol. 185, no. 3, pp. 359–381, 2008.

[2] S. C. Gandevia, K. M. Refshauge, and D. F. Collins, "Proprioception: peripheral inputs and perceptual interactions," *Sensorimotor Control of Movement and Posture*, pp. 61–68, 2002.

[3] C. Bard, M. Fleury, N. Teasdale, J. Paillard, and V. Nougier, "Contribution of proprioception for calibrating and updating the motor space," *Canadian Journal of Physiology and Pharmacology*, vol. 73, no. 2, pp. 246–254, 1995.

[4] A. Tsay, G. Savage, T. Allen, and U. Proske, "Limb position sense, proprioceptive drift and muscle thixotropy at the human elbow joint," *The Journal of Physiology*, vol. 592, no. 12, pp. 2679–2694, 2014.

[5] A. R. Karduna and R. L. Sainburg, "Similarities in the neural control of the shoulder and elbow joints belie their structural differences," *PLOS One*, vol. 7, no. 10, p. e45837, 2012.

[6] J. King, E. Harding, and A. Karduna, "The shoulder and elbow joints and right and left sides demonstrate similar joint position sense," *Journal of Motor Behavior*, vol. 45, no. 6, pp. 479–486, 2013.

[7] C. T. Fuentes and A. J. Bastian, "Where is your arm? variations in proprioception across space and tasks," *Journal of Neurophysiology*, vol. 103, no. 1, pp. 164–171, 2010.

[8] P. Janwantanakul, M. E. Magarey, M. A. Jones, and B. R. Dansie, "Variation in shoulder position sense at mid and extreme range of motion," *Archives of Physical Medicine and Rehabilitation*, vol. 82, no. 6, pp. 840–844, 2001.

[9] M. Allegrucci, S. L. Whitney, S. M. Lephart, J. J. Irrgang, and F. H. Fu, "Shoulder kinesthesia in healthy unilateral athletes participating in upper extremity sports," *Journal of Orthopaedic & Sports Physical Therapy*, vol. 21, no. 4, pp. 220–226, 1995.

[10] R. Blasier, J. Carpenter, and L. Huston, "Shoulder proprioception. effect of joint laxity, joint position, and direction of motion." *Orthopaedic Review*, vol. 23, no. 1, pp. 45–50, 1994.

[11] R. Barrack, H. Skinner, M. Brunet, and S. Cook, "Joint laxity and proprioception in the knee," *The Physician and Sportsmedicine*, vol. 11, no. 6, pp. 130–135, 1983.

[12] T. Aydin, Y. Yildiz, İ. Yanmis, C. Yildiz, and T. A. Kalyon, "Shoulder proprioception: a comparison between the shoulder joint in healthy and surgically repaired shoulders," *Archives of Orthopaedic and Trauma Surgery*, vol. 121, no. 7, pp. 422–425, 2001.

[13] L. A. Hall and D. McCloskey, "Detections of movements imposed on finger, elbow and shoulder joints." *The Journal of Physiology*, vol. 335, no. 1, pp. 519–533, 1983.

[14] S. Scott and G. Loeb, "The computation of position sense from spindles in mono- and multiarticular muscles," *Journal of Neuroscience*, vol. 14, no. 12, pp. 7529–7540, 1994.

[15] N. H. Bhanpuri, A. M. Okamura, and A. J. Bastian, "Predictive modeling by the cerebellum improves proprioception," *Journal of Neuroscience*, vol. 33, no. 36, pp. 14 301–14 306, 2013.

[16] M. P. Boisgontier and S. P. Swinnen, "Proprioception in the cerebellum," *Frontiers in Human Neuroscience*, vol. 8, 2014.

[17] B. L. Tripp, T. L. Uhl, C. G. Mattacola, C. Srinivasan, and R. Shapiro, "Functional multijoint position reproduction acuity in overhead-throwing athletes," *Journal of Athletic Training*, vol. 41, no. 2, p. 146, 2006.

[18] J. Chapman, D. N. Suprak, and A. R. Karduna, "Unconstrained shoulder joint position sense does not change with body orientation," *Journal of Orthopaedic Research*, vol. 27, no. 7, pp. 885–890, 2009.

[19] S. P. Dukelow, T. M. Herter, K. D. Moore, M. J. Demers, J. I. Glasgow, S. D. Bagg, K. E. Norman, and S. H. Scott, "Quantitative assessment of limb position sense following stroke," *Neurorehabilitation and Neural Repair*, vol. 24, no. 2, pp. 178–187, 2010.

[20] L. Rincon-Gonzalez, C. A. Buneo, and S. I. H. Tillery, "The proprioceptive map of the arm is systematic and stable, but idiosyncratic," *PLOS One*, vol. 6, no. 11, p. e25214, 2011.

[21] J. Gordon, M. F. Ghilardi, and C. Ghez, "Impairments of reaching movements in patients without proprioception. I. Spatial errors," *Journal of Neurophysiology*, vol. 73, no. 1, pp. 347–360, 1995.

[22] I. Cusmano, I. Sterpi, A. Mazzone, S. Ramat, C. Delconte, F. Pisano, and R. Colombo, "Evaluation of upper limb sense of position in healthy individuals and patients after stroke," *Journal of Healthcare Engineering*, vol. 5, no. 2, pp. 145–162, 2014.

[23] Y. Rossetti, C. Meckler, and C. Prablanc, "Is there an optimal arm posture? deterioration of finger localization precision and comfort sensation in extreme arm-joint postures," *Experimental Brain Research*, vol. 99, no. 1, pp. 131–136, 1994.

[24] P. Cordo, L. Carlton, L. Bevan, M. Carlton, and G. Kerr, "Proprioceptive coordination of movement sequences: role of velocity and position information," *Journal of Neurophysiology*, vol. 71, no. 5, pp. 1848–1861, 1994.

[25] S. P. Dukelow, "Potential of robots as next-generation technology for clinical assessment of neurological disorders and upper-limb therapy," *Journal of Rehabilitation Research and Development*, vol. 48, no. 4, p. 335, 2011.

[26] F. Conti, F. Barbagli, R. Balaniuk, M. Halg, C. Lu, D. Morris, L. Sentis, J. Warren, O. Khatib, and K. Salisbury, "The CHAI libraries," in *Proceedings of Eurohaptics*, 2003, pp. 496–500.

[27] N. Hoseini, B. M. Sexton, K. Kurtz, Y. Liu, and H. J. Block, "Adaptive staircase measurement of hand proprioception," *PLOS One*, vol. 10, no. 8, p. e0135757, 2015.

[28] G. Schweigart, R.-D. Chien, and T. Mergner, "Neck proprioception compensates for age-related deterioration of vestibular self-motion perception," *Experimental Brain Research*, vol. 147, no. 1, pp. 89–97, 2002.

[29] J. Gordon, M. F. Ghilardi, S. E. Cooper, and C. Ghez, "Accuracy of planar reaching movements," *Experimental Brain Research*, vol. 99, no. 1, pp. 112–130, 1994.

[30] S. H. Scott, "Optimal feedback control and the neural basis of volitional motor control." *Nature Reviews Neuroscience*, vol. 5, no. 7, 2004.

[31] E. Todorov, M. I. Jordan, *et al.*, "Optimal feedback control as a theory of motor coordination," *Nature Neuroscience*, vol. 5, no. 11, pp. 1226–1235, 2002.

[32] J. W. Krakauer, M.-F. Ghilardi, and C. Ghez, "Independent learning of internal models for kinematic and dynamic control of reaching." *Nature Neuroscience*, vol. 2, no. 11, 1999.

[33] N. Colonnese and A. M. Okamura, "Propagation of joint space quantization error to operational space coordinates and their derivatives," in *IEEE/RSJ International Conference on Intelligent Robots and Systems*, 2017, pp. 2054–2061.

[34] R. A. Johnson, D. W. Wichern, *et al.*, *Applied multivariate statistical analysis*. Prentice-Hall New Jersey, 2014, vol. 4.

[35] J. Kalaska, D. Cohen, M. Prud'Homme, and M. Hyde, "Parietal area 5 neuronal activity encodes movement kinematics, not movement dynamics," *Experimental Brain Research*, vol. 80, no. 2, pp. 351–364, 1990.

[36] M. Prud'Homme and J. F. Kalaska, "Proprioceptive activity in primate primary somatosensory cortex during active arm reaching movements," *Journal of Neurophysiology*, vol. 72, no. 5, pp. 2280–2301, 1994.